JOURNAL OF MATERIALS SCIENCE **38** (2003) 1917– 1924

Preparation and structural properties of Cu-Zn-Al-oxides: a comparative study between the hydrodynamic-cavitational and classical route

J. FIND*
Technical University of Munich, Lehrstuhl II für Technische Chemie, Lichtenbergstr.4, D-85747 Garching, Germany
E-mail: Josef.Find@ch.tum.de

W. R. MOSER
Department of Chemical Engineering, Worcester Polytechnic Institute, 100 Institute Road, Worcester, MA, 01609 USA

Series of Cu-Zn-Al oxides have been prepared using a mixture of aqueous Na_2CO_3 and NaOH solutions for precipitation to investigate the influence of these agents on the formation of the precipitates and, subsequently, on the structure of the oxides. Two synthesis routes are applied, one classical in a well stirred beaker and a second one using a cavitational device. Differences in phase compositions, crystallite sizes and strain are observed for the calcined materials. One further series was performed varying solvent, precipitation agents and pH. The controlled production of crystallite sizes in a range from 5 to 10 nm and the insertion of strain into the material have been verified. The cavitational preparation route offers new fundamental insights in the formation of this important mixed oxide system and favours investigations in direction of the design of nanoscopic materials. The results are discussed in terms of cavitational effects and compared to results obtained from classical experiments.

1. Introduction

In recent years high shear hydrodynamic cavitation has been reported as an impressive alternative synthesis pathway [1–4] for nano-phase materials in large quantity and high phase purity compared to classical co-precipitation methods. Cavitation, the formation of vapour gas bubbles in a liquid caused by a reduction in pressure at constant temperature, is well known in engineering sciences. e.g., rapid movements of propeller blades in liquids or pistons in pumps suffer on extreme pressure drops forming cavities, which might damage the devices. From another point of view enormous energies can be released as shock waves or local temperature rise, which might be useful for the synthesis of materials. Temperatures up to 5000 K resulting from cavitation are reported [5–7], which should generate an *in situ* calcination of the hydroxides to form metal oxides. The creation of cavitation itself is strongly dependent on the design and the geometry of any device used and the experimental parameters. For this work the laboratory model CaviPro^{TM} of Five Star Technologies^{TM} is used to form cavitation. The system Cu-Zn-Al was chosen as example because it is well known that in this system the synthesis procedure affects enormously the structural properties of the formed material [8]. Cu-Zn-Al mixed oxides are industrial catalysts for methanol synthesis and syn-gas synthesis. Both processes demand reduced Cu particles in high dispersion, which is in general obtained by a synthesis strictly depending on the adjustment of pH, concentration, synthesis temperature and aging (crystallization time) of the slurry. A variety of preparation conditions were tested e.g., solvent, precipitation agent and anion concentration (OH^-, CO_3^{2-}) to investigate the different structural characteristics of the synthesized materials prepared by the cavitational device and by classical co-precipitation. The comparison of these two preparation routes should, therefore, allow new insights in the mechanism and formation of these materials. In this work the variation of nano-scale based structural properties such as strain and controlled growth of the crystallite size was of special interest. Strain in a solid can be understood as 3-dimensional solid-state defect. Therefore, small crystallites with a high amount of defects are an interesting material for catalytic applications.

Hydrodynamic cavitation is not limited to the synthesis of mixed oxide catalysts only. Bi-functional catalysts, supported metal catalysts and complex metal oxides ceramics are reported [9], which have been prepared successfully in nano-structured grains and high phase purity.

* Author to whom all correspondence should be addressed.

TABLE I Diameters of the orifices used for the syntheses in the CaviPro^{TM}. The flow was kept constant at 350 ml/min

Diameter (mm)	Pressure (MPa)
1st orifice/no.	
0.152/1	168.5
0.178/2	97.6
0.203/3	68.5
0.254/4	34.3
0.305/5	19.2
2nd orifice	
0.356/6	–

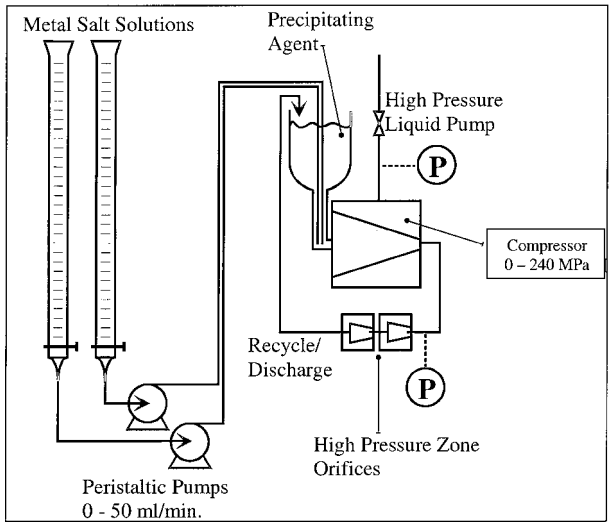

Figure 1 Schematic drawing of the experimental setup.

2. Experimental

The device CaviPro^{TM} [9, 10] of Five Star Technologies^{TM} was used for the hydrodynamic cavitation preparation, which represents an optimised device to generate a maximum yield of cavitation events. The advantage of this device is the formation of cavitation under high flow and high pressure conditions. The flow rate, pressure and orifice size are adjustable parameters, which allow mechanically to control the synthesis of materials. Different sets of orifice pairs were used to allow the mechanical variation of flow conditions and inlet pressure. Table I summarizes the mechanical parameters used for the cavitational preparation series. A schematic drawing of the experimental set-up is given in Fig. 1. A detailed description of the experiments is given in the next paragraph. Classical precipitations were performed in a beaker with a high power stirrer.

The X-ray diffraction experiments (XRD) were done in Bragg-Brentano geometry (reflection mode; graphite-secondary monochromator, Cu K_α-radiation, $\lambda = 154.16$ pm) with a Rigaku Geigerflex diffractometer. The program *PowderCell* [11] was used to deconvolute phase mixtures and to simulate their X-ray patterns.

3. Sample preparation

The metal salt solution was prepared by dissolving 0.1 mol $Al(NO_3)_3 * 9H_2O$, 0.25 mol $Cu(NO_3)_2 * 3H_2O$ and 0.65 mol $Zn(NO_3)_2 * XH_2O$ in 1000 ml deionised water. As precipitation agents 1 molar Na_2CO_3, NaOH and $(NH_4)_2CO_3$ aqueous solutions were used. At the start of a typical cavitational experiment, the device was turned on to begin recirculation of the solvent, which consisted of 300 ml of water or isopropanol. Once the solvent was flowing through the system, two process streams, one containing 50 ml of the metal solution and one 50 ml of the precipitation agent, were introduced into the experimental set-up using precision peristaltic pumps. The formed precipitate solution flowed through the orifice section and was continuously recirculated throughout the addition of the feed streams (10 min), followed by additional recirculation of 20 min. The temperature of the recirculating material was regulated to 303 K by cooling the solution through the use of an in-line heat exchanger. At the end of a synthesis, the product slurry was collected and then pressure filtered under 0.67 MPa of nitrogen using 142 mm diameter, 0.2 μm nylon filter paper. After the initial pressure filtration, the filter cake was washed and re-filtered. The washed solid was then dried overnight (at least 12 hrs) at 373 K. The dried materials were calcined at 623 K for 4 hrs. Classical experiments were performed analogously at 333 K, at a constant pH of 7 and under continuous stirring for 30 min.

4. Results

4.1. Influence of the anion

Two series of four samples, prepared by the cavitational and the classical route, were performed using 50 ml of a mixture of 1 M Na_2CO_3 with 1 M NaOH solution as precipitation agents. In the following these samples are called '*CP*' for classical, and '*Cav*' for the cavitational prepared materials. The number accompanying expresses the mixtures of precipitation solutions, which is equivalent to 'mol% NaOH' used. e.g., CP33 is the abbreviation for a classical experiment using 33 mol% of NaOH and 67 mol% of Na_2CO_3. The orifice set 1–6 was used with a constant inlet pressure of 137.9 MPa. The XRD patterns of the dried materials are compiled in Fig. 2 with the patterns of Cav0, Cav33, Cav66 and Cav100 in the upper and of CP0, CP33, CP66 and CP100 in the lower part. $Cu_4(NO_3)_2(OH)_6$, isostructural to the mineral 'Gerhardtite' [12] was identified as crystalline compound in Cav100, Cav66 and Cav33, while in the classically prepared samples only in CP100. The crystallinity of Gerhardtite in the cavitational samples prepared is much higher combined with a preferred orientation along the [00/]-direction. This is obvious comparing the intensity ratio of the sharp reflections (002) and (004) with the lines (200), (120) and (202). In CP100 the single lines can still be referred, while for the samples prepared in the cavitational device only the (002) and the (004) reflections are very sharp, but the lines in the range from 32 to 38 2Θ are observed as one asymmetric broad hump. In both preparation series additionally a pair of broad lines is observed at 10 and 22 2Θ. This compound was not identified, but is similar in its shape and pattern to distorted layered structures like known in graphite intercalation compounds [13] or clays. With higher concentration in CO_3^{2-} the patterns of Gerhardtite are decreasing in

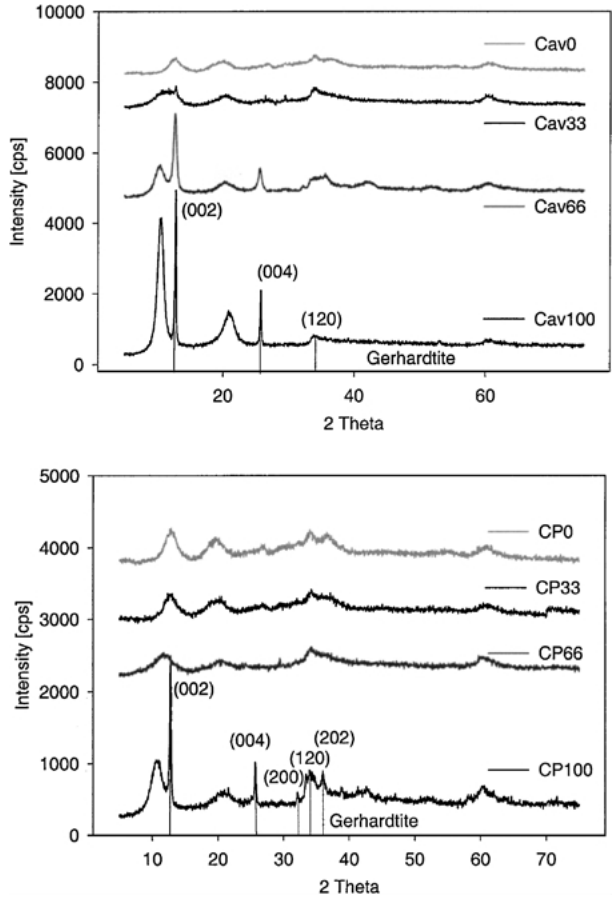

Figure 2 The upper part shows the XRD pattern of the dried cavitational samples the lower part that of the classical. The NaOH mol% in the precipitation solution is indicated for each pattern. With higher amount of NaOH the formation of Gerhardtite is observed.

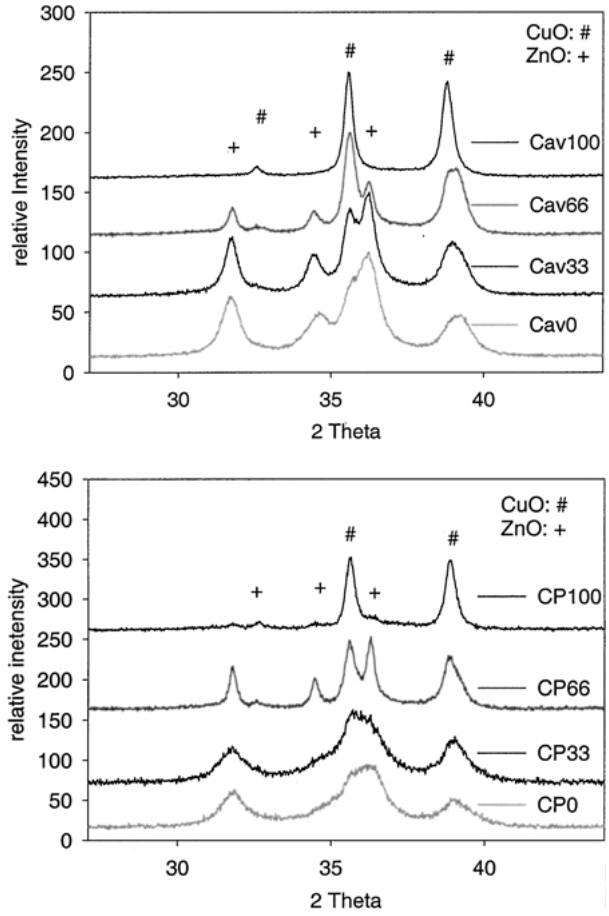

Figure 3 After calcination at 623 K for four hours two crystalline phases, CuO and ZnO are detected. The upper part shows the XRD pattern of the cavitational samples, the lower part that of the classical. The amount of ZnO is increasing with decreasing NaOH concentration. The crystallite size of CuO is correlated to the amount of Gerhardtite detected in the dried samples.

the cavitational samples indicated by line broadening of (002) and (004). Furthermore, in both series the unknown phase disappears indicated by the disappearance of the broad lines at 10 and 22 2Θ, while in the samples Cav100 and CP100 broad lines of a different phase are observed. Additionally, the signal-to-noise ratio increases with increasing CO_3^{2-} concentration indicating that all compounds became more X-ray amorphous. Fig. 3 reveals the X-ray patterns of the materials calcined at 623 K for four hrs. Two crystalline phases were detected, CuO and ZnO. Again, with a lower concentration in OH^-, the observed patterns reveal broader lines. The change in the phase composition as a function of the concentration of NaOH used in the preparation is shown in Fig. 4. For both series a linear increase of the amount of detected CuO was observed with increasing NaOH concentration. In parallel the total yield in oxide produced was decreasing. Comparing the patterns of the calcined samples to those of the dried materials, there is a strong indication that the crystallite size of CuO in the calcined samples is correlated with the higher amount of Gerhardtite detected in the dried samples, as the crystallite size is increased.

While in the CP100 ZnO and CuO were detected, only CuO was identified in Cav100. In the CP0 and Cav0 samples the ratio of phase composition between CuO and ZnO was 1:3 and 1:2 for the classical and the cavitational sample. To understand this difference in composition, all samples were washed again with deionized water respectively to allow a recrystallisation and the formation of Hydrotalcite, $Cu_xZn_{6-x}Al_2(OH)_{16}CO_3 * 4H_2O$, as reported by Prinetto and co-workers [8]. Fig. 5 reveals the XRD patterns of the washed samples. The phase composition of these samples before and after the washing procedure

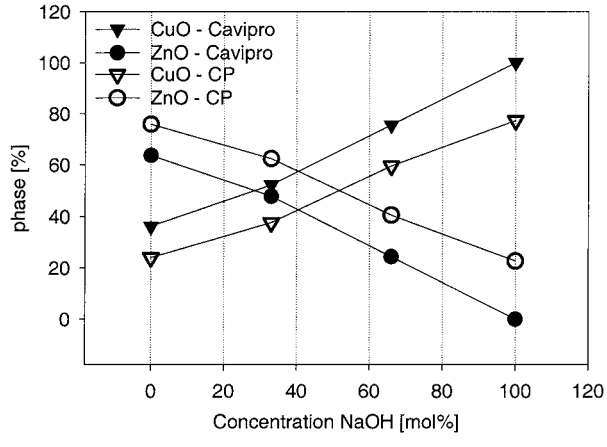

Figure 4 The phase composition detected by XRD is correlated linearly to the concentration of NaOH used in the precipitation. For the Cavipro experiments a general shift is observed. The amount in CuO is higher and the amount in ZnO is lower than in the corresponding classical experiments.

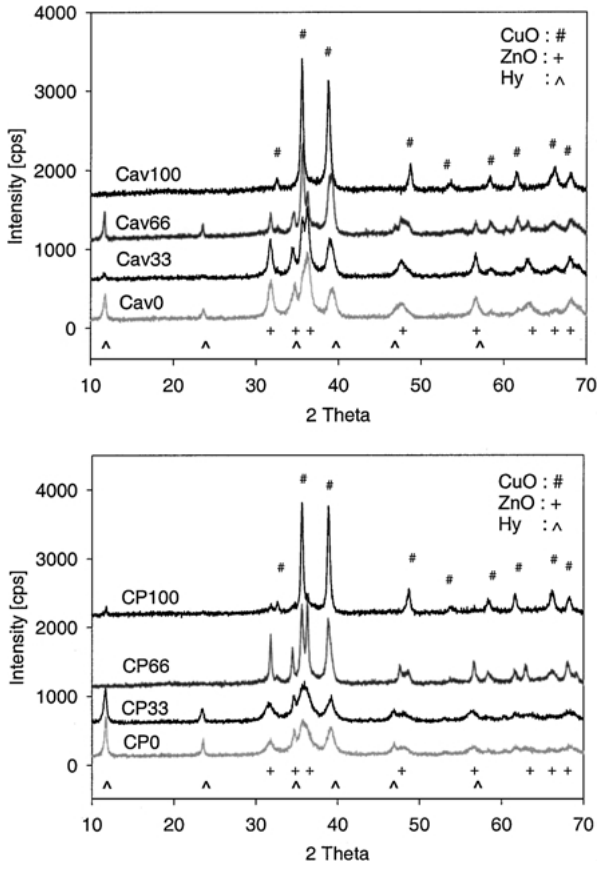

Figure 5 After washing the samples additionally hydrotalcite has been detected by XRD as reported [8]. The upper part shows the Cavipro, the lower part the classical samples. With increasing amount of NaOH the amount of hydrotalcite is decreased. Furthermore, the concentration in hydrotalcite is much higher in the classical samples comparing the corresponding Cavipro samples.

is given in Table II. Hydrotalcite was primarily found in the samples precipitated with a higher amount of carbonate. Furthermore, it has been observed that the lattice parameters of Hydrotalcite were different comparing both series. Table III compares our data obtained for Cav0 and CP0 with the data reported by Busetto [14], who investigated the crystal structure of Hydrotalcite in dependence on the Cu and Zn concentration. We can conclude that in the classical preparation the ratio between incorporated Cu and Zn ions is 1:3 (with $x = 1.4$), while the cavitational produced sample contains almost no copper ($x = 0.2$). This result explains, why the ratio of free CuO to ZnO in the calcined Cav0 (1:2) is larger than it is theoretically possible, while the classical CP0 represents the stoichiometric ratio 1:3 from the starting metal solution. Comparing the patterns of the washed samples with the patterns of the calcined samples it is remarkable that the only detectable difference is the additional appearance of the phase Hydrotalcite. No detectable structural changes are observed for CuO and ZnO after the washing procedure.

TABLE III Cu content in Hydrotalcite detected in comparison with data reported by Busetto [15]

Hydrotalcite $Cu_xZn_{6-x}Al_2(OH)_{16}CO_3 * 4H_2O$		
	Our data	
Exp	x/Cu:Zn	c-axis
Cav100	0.2/3.33	22.78
CP100	1.4/23.33	22.68
	Busetto [15]	
	0/0	22.80
	2/33.33	22.62

Strain analyses by the method of Williamson and Hall [15] and crystallite size determination using the Debye-Scherrer equation were performed. In Fig. 6 strain and crystallite size are shown as a function of the NaOH concentration. The strain analyses revealed that the cavitational samples revealed much higher strain with decreasing particle size than the classical samples. An increase in strain by cavitational synthesis has already been reported [9] for TiO_2 and Pb (Zr, Ti) O_3 mixed oxides. It has been found that the introduction of strain is correlated to the Reynolds and the Cavitation number and can therefore be used by adjusting pressure and orifice set to predict the amount of strain to expect. The crystallite size and the strain for CuO, the total yield and the concentration in NaOH are summarized in Table IV. The same tendencies in strain and crystallite size are observed for ZnO, but in much less extent.

4.2. Influence of solvent and precipitation agent

A second set of four experiments was performed in analogy to the series described above varying pressures

TABLE II Phase compositions of the cavitational and the classical experiments in dependence on the precipitation solution mixture for and after washing

	Calcined (mol%)		Calcined + washed (mol%)		
NaOH (mol%)	CuO	ZnO	CuO	ZnO	Hydro-talcite
		Cavitational experiments			
100	100.0	0.0	100.0	0.0	0.0
66	77.2	22.8	65.1	19.2	15.7
33	52.2	47.8	45.7	50.2	4.1
0	36.3	63.7	29.6	51.9	18.5
		Classical experiments			
100	77.9	22.1	76.0	21.5	2.5
66	62.5	37.5	62.5	37.5	0.0
33	37.6	62.4	28.3	47.0	24.7
0	24.1	75.9	18.0	56.7	25.3

TABLE IV Crystallite size and strain of CuO as function of the NaOH concentration used in the precipitation. Additionally the total yield in oxides is given

	CuO size (nm)		CuO strain (%)		Total yield in oxides (%)	
NaOH (mol%)	CaviPro™	Classical	CaviPro™	Classical	CaviPro™	Classical
100	25.8	25.9	0.56	0.37	34.9	50.5
66	19.6	15.7	1.76	0.74	45.1	70.5
33	13.4	9.7	2.32	0.68	70.8	76.7
0	11.8	9.0	2.99	0.78	89.7	92.3

and orifice sets (see Table I) at a constant flow of 350 ml/min to investigate the influence of the solvent isopropanol ('*IPA*'▲) or water ('H_2O-7'●) and of the precipitation agents Na_2CO_3 ('H_2O-7') and $(NH_4)_2CO_3$ ('NH_4^+'▼) at a pH of 7. The initial pressure in front of the first orifice is given in Table I. One precipitation with a 1 M aqueous Na_2CO_3 solution was done at pH ∼ 9 ('H_2O-9'♦) to investigate the influence of pH on the structure of the oxides. The abbreviation term for each series is given in *italics* naming the varied parameter. Fig. 7 reveals the results of the strain and crystallite size analysis of CuO in the upper and of ZnO in the lower part. For comparison the data of the classical experiments are plotted in filled symbols. In Fig. 8 the crystallite size of CuO is given as function of the orifice size in the upper part and in the lower part that obtained for the strain in CuO.

For CuO it has been found that the strain is varied between 0.7 and 2.3% depending on the chosen orifice set, while the crystallite size varies in a range from 6 to 9 nm. The highest amount of strain is found for *IPA*, followed by H_2O-7. The smallest strain was detected in NH_4^+, while H_2O-9 showed no influence, neither on strain nor on size. The classical experiments led to a crystallite size of 9 nm for *IPA*, H_2O-7 and H_2O-9, while in NH_4^+ the smallest crystallite size of 4 nm was detected. In *IPA* and H_2O-7 a strain of ∼0.8% and in H_2O-9 and NH_4^+ of 1.4% was determined. Furthermore, it is clear from the data shown in Fig. 8 that the maximum in strain and the minimum in crystallite size are not linearly correlated to the orifice size. The largest strain and the smallest crystallite size in CuO were found in the cavitational experiment using the orifice set 4–6.

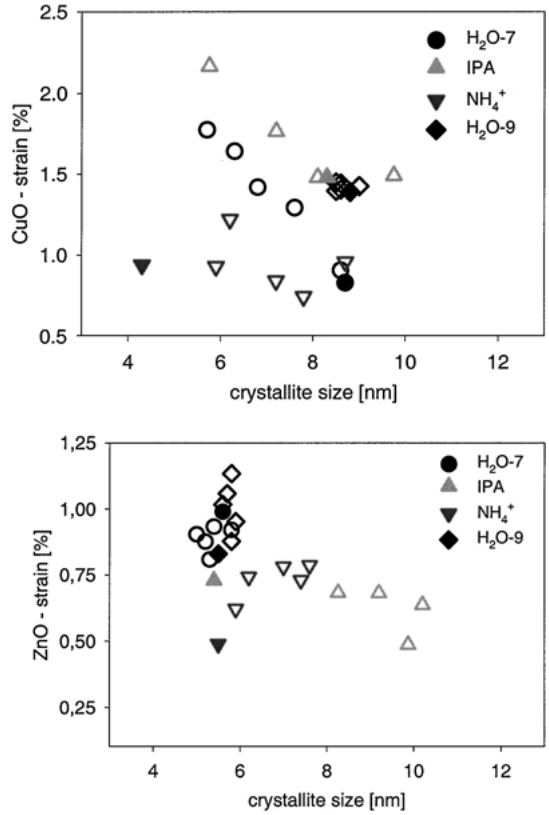

Figure 7 The Cavipro can be used to control the crystallite size of CuO (upper plot) and ZnO (lower plot) by varying mechanical parameters. The classical experiments are marked with closed symbols, the Cavipro experiments in open symbols. The highest strain in CuO has been observed using Na_2CO_3 in IPA, the lowest strain in the precipitation with $(NH_4)_2CO_3$ in water. ZnO did not show those significant changes. Here, the strain was almost constant for each experiment, while the main influence was detected for the crystallite size.

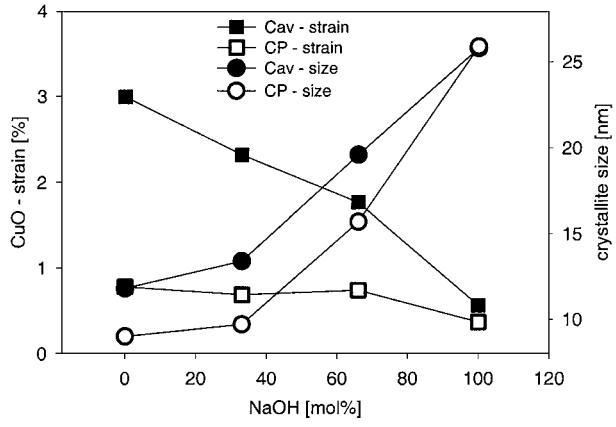

Figure 6 With increasing NaOH concentration the crystallite size is increased. Even though the crystallites observed in the classical samples are smaller, the strain detected is larger in the Cavipro samples.

For ZnO the observed crystallite sizes can be separated in three regions. Here, H_2O-7 and H_2O-9 and all classical experiments led to crystallites of about 5 nm. NH_4^+ led to crystallites between 6 to 8 nm and *IPA* between 8 to 10 nm. The strain difference detected was much less than in the CuO. H_2O-7 revealed an average strain of about 0.9%, while the average strain of NH_4^+ and *IPA* was about 0.7%. Only H_2O-9 revealed a slight variation in strain ranging from 0.8 to 1.2%. In the classical experiments the highest strain of 1% was detected for H_2O-7, while that of H_2O-9 and *IPA* was about 0.75%. The lowest strain of 0.5% was detected in NH_4^+.

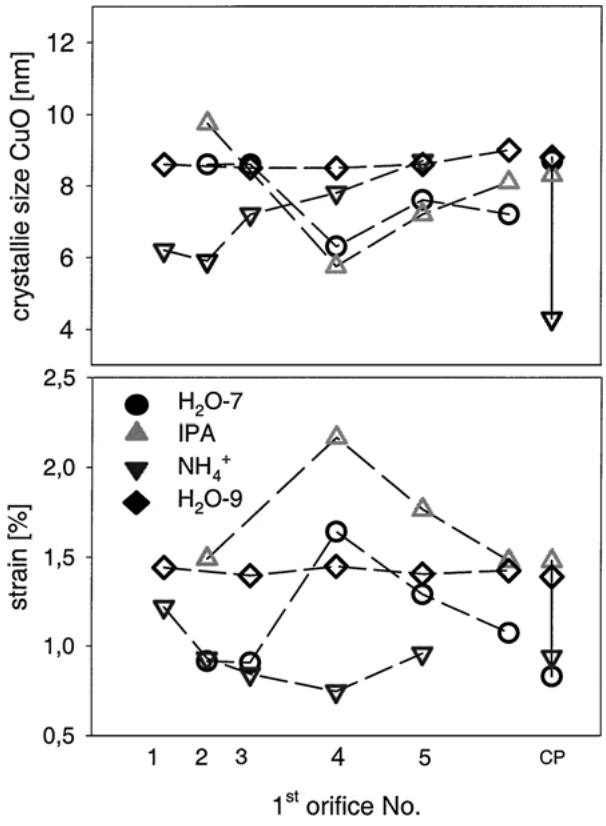

Figure 8 The changes in crystallite size (upper plot) and in strain (lower plot) in CuO are not linearly correlated to the orifice size. A smallest crystallite size and a highest strain are observed for the experiment performed with the orifice with a diameter of 0.25 mm.

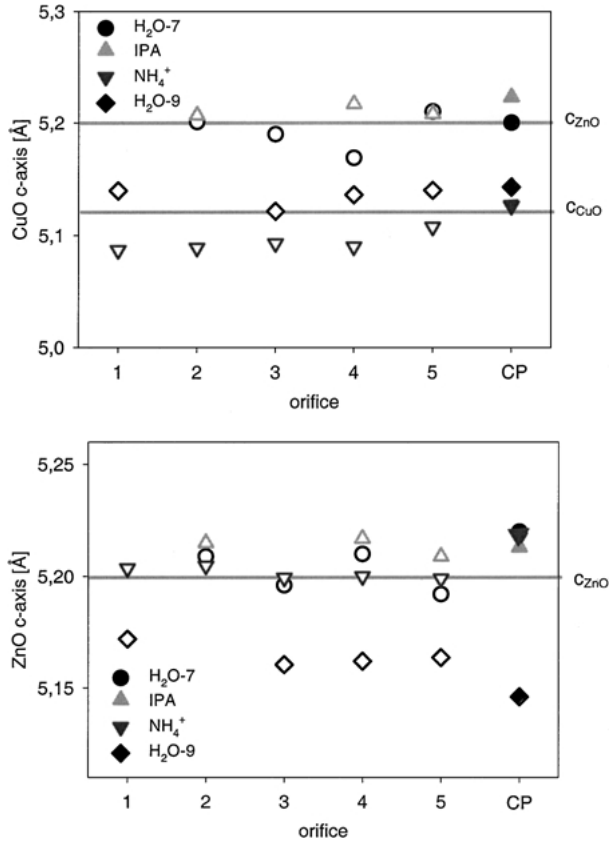

Figure 9 The lattice parameters for CuO and ZnO have been analysed. For CuO the precipitation at pH = 7 with Na_2CO_3 in IPA or water a shift in the *c*-axis into the direction of the *c*-axis of ZnO is observed. For ZnO a shift of the *c*-axis into the direction of CuO has been detected for the precipitation at pH = 9 with Na_2CO_3 in water.

The detected length of the *c*-axis of CuO and ZnO are summarized in Fig. 9 as we observed there a shift for CuO and ZnO. The observed values of the *c*-axis for CuO and ZnO are given in dependence on the orifice size. The *c*-axis values of single crystal data of both phases [16, 17] are shown as full line. Note that the classical experiment is also included at the right side on the plots marked by filled symbols. A shift in the *c*-axis of CuO (upper plot) from 5.12 to 5.20 Å was observed for *IPA* and H_2O-7. This value of the CuO-*c*-axis is identically with the value of the *c*-axis of ZnO. For *H_2O-9* a shift of the *c*-axis of ZnO (lower plot) into the direction of the *c*-axis of CuO from 5.20 to 5.16 Å has been observed. In NH_4^+ no changes in the lattice constants were observed in respect to CuO and ZnO. The same shifts were detected in the classical samples. Therefore, we can conclude that these shifts are not caused by hydrodynamic cavitation, but by chemical procedure.

As a consequence we can conclude that strain and crystallite size can be varied by changing the mechanical parameters of the cavitational device. This variation (compare Fig. 8 crystallite size and orifice diameter) allows also for Cu-Zn-Al mixed oxides the controlled adjustment of solid state characteristics.

5. Conclusions

In the first part it has been shown that the comparison of the classical with the hydrodynamic-cavitational synthesis allows new insights in the formation of ternary Cu-Zn-Al oxides. The variation in the ratio of CO_3^{2-} and OH^- led to different phase compositions comparing the cavitational to the classical synthesis as demonstrated in Fig. 4 and Table II. We have shown that the anion concentration of CO_3^{2-} and OH^- has an enormous influence on the precipitates and the calcined oxides. With increasing concentration in CO_3^{2-} the crystallite size of the material in the dried and calcined state became smaller. This is in agreement with the decreasing amount in CuO observed in XRD (compare Fig. 3 and Tables II and IV) and in parallel with the decrease in the total yield of oxide and thus the decreasing phase contingent in ZnO. Furthermore, it was shown that under the cavitational conditions applied the high pressure stabilizes the formation and crystallization of Gerhardtite, $Cu_4(NO_3)_2(OH)_6$, which leads to the formation of larger CuO crystallites after calcination. The expected *in situ* calcination caused by cavitation was not observed. In Fig. 2 the patterns of CP100 and Cav100 reveal a mixture of crystalline Gerhardtite and at least one unknown phase. The broad lines at 10 and 22 2Θ are typically for XRD patterns observed on layered materials [13, 18]. These materials are distinguished for a two-dimensional long range order indicated by belonging intense lines, while the third direction has only a short range ordering and, therefore, the belonging lines have only weak intensities. The intensities of those lines disappear, and so the amount on this unknown phase with decreasing amount of OH^-. Therefore, we suggest that this unknown phase is a layered hydroxo-phase. With increasing concentration in CO_3^{2-} the amount of OH^--rich

Gerhardtite, $Cu_4(NO_3)_2(OH)_6$, is decreasing. A new material is formed, which we could not identify. The different XRD line positions exclude Gerhardtite and Hydrotalcite in a less crystalline state. Additionally, the amount on ZnO detected in the calcined samples increased. In conclusion it is evident that CO_3^{2-} stabilize the precipitation of Cu^{2+}, Zn^{2+} and Al^{3+} cations. The distribution and the size of the CuO crystallites is determined firstly by the crystallinity of the formed precursor Gerhardtite and is secondly related to the total yield of oxides formed. The crystallite size of CuO was in average smaller in the classical preparations, where Gerhardtite is found only in CP100. The third parameter, which controls the crystallite size of CuO, is the insertion grade of Cu^{2+} into the structure of Hydrotalcite, which crystallises after washing the calcined oxides. In the classical samples much more Cu^{2+} is located in Hydrotalcite, $Cu_xZn_{6-x}Al_2(OH)_{16}CO_3 * 4H_2O$, with $x = 1.4$, where in the cavitational sample x was determined to 0.2. This circumstance shifts the CuO:ZnO ratio, in the classical samples determined to 1:3, to 1:2 in the cavitational samples. Furthermore, it has been found that by cavitational synthesis strain can be introduced in materials. This is in agreement with the observations made for other (mixed) oxide systems mentioned already at the end of the last paragraph.

In the second part preparation series are reported investigating the possibilities to control structural properties by the use of the cavitational device. Here, different preparation parameters e.g., the solvent (isopropanol or water) the precipitation agent and the pH and the orifice sets were varied and its influence on the structural properties was investigated. It has been found that CuO is most sensitive to the cavitational parameters pressure, orifice size and flow conditions. The correct adjustment of these parameters allows the variation of crystallite size in a range from 6 to 10 nm with the parallel insertion of strain into the material. The smaller the crystallite size the larger the strain detected. The highest strain was found for *IPA*, while the smallest strain was detected in NH_4^+. The preparation performed at pH ~ 9 allowed neither variation in crystallite size nor in strain. These results can be explained taking into account the morphology and the solvability of the precipitate. Preparation at a pH of 7 led in all experiments to a powder, the preparation at pH 9 to a gel. After drying and calcining the gel no induced hydrodynamic-cavitational modifications remain. So, decomposition and re-crystallization processes are prevailing. Therefore, all resulting oxides have the same properties. Precipitation with $(NH_4)_2CO_3$ at pH ~ 7 is influenced by the cation NH^{4+}, which forms complexes e.g., a $Cu(NH_3)_4^{2+} * 2\,H_2O$-complex in solution. These complexes make the precipitation of the forming Cu-species difficult. However, to produce smaller CuO crystallites the complexation of Cu^{2+} by NH_3 is helpful to increase the dispersion. Precipitation in IPA accelerates the growth of the freshly formed precipitates, because the metal precipitates are less soluble in IPA than in water. Therefore, we can conclude that a lower solvability is better to introduce strain, especially into CuO.

The cavitational modification in strain for CuO follows the sequence:

$$IPA > H_2O\text{-}7 > H_2O\text{-}9 > NH_4^+$$

Furthermore, it has been observed that changes in crystallite size and strain are not linearly correlated to the diameter of the orifices. The ultimate values are found for the orifice set 4–6. Therefore, we can conclude that the use of this orifice is the most appropriate to achieve the smallest crystallite size and a maximum in strain under the conditions supplied. But for other experimental conditions or other chemical systems, it might be that another orifice is more efficient. This result shows clearly that applying the cavitational preparation for the synthesis of inorganic materials is a very complex method, where cavitation and fluid dynamics are interacting strongly with each other.

The properties of ZnO were also modified. The highest strain of about 1% was detected in H_2O-*7* and H_2O-*9* without any change in the crystallite size ($\sim$5 nm). The strain in the series *IPA* and NH_4^+ had an average value of 0.7% but a wider range in crystallite sizes 8 to 10 nm and 6 to 8 nm respectively. The strain increased for ZnO in the sequence:

$$H_2O\text{-}9 > H_2O\text{-}7 > NH_4^+ > IPA$$

Comparing the classical preparations to the cavitational experiments no change in the crystallite size was detected for ZnO.

Additionally, variations in the lattice parameters are detected. H_2O-*7* and *IPA* revealed an extension in the *c*-axis of CuO from 5.12 to 5.20 Å. H_2O-*9* revealed a shorter *c*-axis of ZnO decreased from 5.20 to 5.16 Å. For NH_4^+ the reported axes lengths of pristine CuO and ZnO are detected. These changes are strong indications of different interactions between CuO and ZnO. One possible explanation is the epitaxial growth of one species on the other. Therefore, the shift in the *c*-axis of CuO observed for H_2O-*7* and *IPA* would indicate a preferred growth of CuO on ZnO, while the shift in the *c*-axis of ZnO into the direction of the value of the *c*-axis of CuO observed in H_2O-*9* would indicate a preferred growth from ZnO onto CuO. The comparison with the classical experiments revealed that the changes in the lattice constants are also observed here and, therefore, cannot be the result of the use of the cavitational device. The use of the cavitational device allows the variation of the crystallite size and favours the introduction of strain into the oxides, which should be especially for their catalytic application of enormous importance. Catalytic investigations will be performed to work out the influence of the observed structural characteristics of these materials.

The observed modifications in the lattice constants and in strain are of special interest for a catalytic application. Recently, it has been reported [19] that strain in Cu/ZnO is directly correlated to the turnover-frequency in the methanol synthesis reaction. The higher the strain the more activity has been observed.

Furthermore, it is speculated that epitaxial growth of Cu on ZnO is responsible for the increase in strain. These data are in excellent agreement with the changes in the lattice parameters reported here.

Acknowledgements

The authors wish to thank S. C. Emerson and I. M. Krausz for helpful discussions and Five Star Technologies™ for the financial support and the donation of equipment, which made this work possible.

References

1. W. R. MOSER, B. J. MARSHIK, J. KINGSLEY, M. LEMBERGER, A. CHAN, J. E. SUNSTROM IV and A. BOYE, *J. Mater. Res.* **10**(9) (1995) 2322.
2. W. R. MOSER, US Patent 5,466,646 (1995).
3. *Idem.*, US Patent 5,417,956 (1995).
4. W. R. MOSER, T. GIANG, S. NYGUEN and O. KOZYUK, in "Process Intensification for the Chemical Processing by Controlled Flow Cavitation," Vol. 38, edited by A. Green (BHR Group Publications, 1999) p. 173.
5. K. S. SUSLICK, T. HYEON, M. FANG and A. A. CICHOWLAS, "Elsevier: Materials Science & Engineering A—Structural Materials Properties Microstructure & Processing" (A204, no. 1–2 Switzerland, 1995) p. 186.
6. K. S. SUSLICK, Y. DIDENKO, M. M. FANG, T. HYEON, K. J. KOLBECK, W. B. MCNAMARA III, M. M. MDLELENI and M. WONG, *Phil. Trans. Roy. Soc.* A **357** (1999) 335.
7. W. B. MCNAMARA III, Y. DIDENKO and K. S. SUSLICK, *Nature* **401** (1999) 772.
8. F. PRINETTO, G. GHIOTTI, P. GRAFFIN and D. TICHIT, *Micrp. Mesop. Mater.* **39** (2000) 229.
9. J. FIND, S.C. EMERSON, I. M. KRAUSZ and W. R. MOSER, *J. Mater. Res.* **16**(12) (2001) 3503.
10. O. V. KOZYUK, A. A. LITVINENKO, K. B. K. KRAVETS and V. V. BEREZIN, US Patent 5,492,654 (1996).
11. W. KRAUS and G. NOLTZE "PowderCell for WINDOWS" Version 2.3 (Berlin, Germany, 1999).
12. W. NOWACKI and R. SCHEIDEGGER, *Helv. Chim. Acta* **35** (1952) 375.
13. J. FIND, D. HEREIN, Y. UCHIDA and R. SCHLÖGL, *Carbon* **37**(9) (1999) 1431.
14. C. BUSETTO, G. DEL PIERO, G. MANARA, F. TRIFIRO and A. VACCARI, *J. Catal.* **85** (1984) 260.
15. G. K. WILLIAMSON and W. H. HALL, *Acta Metall.* **1** (1953) 22.
16. S. ASBRINK and L. J. LORRBY, *Acta Cryst.* B **26** (1970) 8.
17. S. C. ABRAHAMS and J. L. BERNSTEIN, *ibid.* B **25** (1969) 1233.
18. M. BELLOTTO, B. REBOURS, O. CLAUSE, J. LYNCH, D. BAZIN and E. ELKAIM, *J. Phys. Chem.* A **100** (1996) 8527.
19. M. M. GÜNTER, T. RESSLER, B. BEMS, C. BÜSCHER, T. GENGER, O. HINRCHSEN, M. MUHLER and R. SCHLÖGL, *Catal. Lett.* **71**(1/2) (2001) 37.

Received 29 July 2002
and accepted 21 February 2003